RSC Advances

ROYAL SOCIETY OF CHEMISTRY

www.rsc.org/advances

Superhard-Driven Search of the Covalent Network in B_3NO System

Qian Li,[1] Jianyun Wang, [1] Miao Zhang,[1,3] Quan Li,[2,1,*] and Yanming Ma,[1]

[1] *State Key Laboratory of Superhard Materials, Jilin University, Changchun 130012, China*

[2] *College of Materials Science and Engineering, Jilin University, Changchun 130012, China*

[3] *College of Physics, Beihua University, Jilin 132013, China*

Abstract

The search of new superhard materials with Vickers hardness larger than 40 GPa remains considerably experimental and theoretical challenges. Here, we perform superhard-driven search using an unbiased structure search method based on CALYPSO method in the ternary B-N-O system, B_3NO, which is isoelectronic with diamond. A variety of newly predicted structures of B_3NO compound with short, strong, and three-dimensional covalent bonds are designed here. Among them, two newly predicted orthorhombic structures with *Imm*2 (oI20) and $Pmn2_1$ (oP20) space group are found to be superhard and energetically stable. After examining the dynamical stabilities, we found that these two structures are energetically more preferable. The further hardness calculations show the two structures are superhard materials with Vickers hardness above 45 GPa, exceeding the criterion of superhard materials. The electronic results show oI20 and oP20 structures are semiconductor materials with optimal band gap of 0.87 and 0.12 eV, respectively. The present results reveal that the B_3NO compounds can be used as superhard material or narrow band-gap semiconductor materials, which have a broad prospect in industrial application, and also provide insights for exploring other functional compounds with functionality-driven design.

1. Introduction

Superhard materials play an important role in a variety of industrial applications, e.g. from cutting, polishing tools to wear-resistant coatings.[1] It is well known that diamond is the hardest known material with a measured hardness from 60 to 120 GPa[2] experimentally. However, it is limited by several shortcomings, including brittleness, easily reacting with iron-containing materials and oxidization in air under high temperature. An immense amount of experimental and theoretical studies have been devoted to searching new superhard materials with greater thermal stability and inert chemical activity.[3-6] Traditionally, it is commonly accepted that superhard materials are formed by light elements (B, C, N and O), since they contain short and strong covalent bonds providing to resist both elastic and plastics deformations. e.g., *c*-BN,[7] C_3N_4,[8] B_2O,[9,10] BC_2N,[11-17] B_2CO[18], and BC_3[19,20]. Note that previous works have already demonstrated that diamond-like superhard *c*-BN[7] and B_2O[9,10] compounds can form typical sp^3 covalent B-N and B-O bonds. It is reasonable to suppose that materials with mixed B-N and B-O bonds may possess covalent bonding network, resulting in high hardness. It is noteworthy that B_3NO has 20 valence electrons per formula unit (4 valence electrons per atom) and is thus isoelectronic with diamond (they have the same valence electrons per atom). Isoelectronic compounds always have similar chemical bonds and structural properties. Therefore, it is expected B_3NO would form typical strong covalent sp^3 bonds, which are necessary conditions for superhard materials.

The search of candidate structures is critical to understand the hardness and related physical properties of B_3NO. In this work, we have predicted various structures for B_3NO under 0 ~ 100 GPa with superhard-driven CALYPSO method, which is a developed methodology to design superhard materials for given chemical systems under high pressure. It is in contrast to the traditional ground-state prediction method where the total energy is solely used as the fitness function. We adopt hardness as the fitness function in combination with the first-principles method to construct the hardness vs. energy map by seeking a proper balance between hardness and energy for a better mechanical description of given chemical systems. We have predicted a plenty variety of structures with high hardness and relatively low energy. Two energetically structures are uncovered in our structure searches consisting of strong

covalent B-B, B-N and B-O bonds. The calculations show they are superhard materials with Vickers hardness above 45 GPa. Our current work significantly improves the understandings of superhard-driven predictions and also reveals that B_3NO behave as both superhard and photocatalytic materials, which have been widely used in industrial implications.

2. Computational Details

Our global structural prediction uses the unbiased intelligence based on CALYPSO (Crystal structure AnaLYsis by Particle Swarm Optimization) method[21-23] which has successfully predicted structures of various systems ranging from elemental solids to binary and ternary compounds.[24-29] The main characteristics of CALYPSO contain functionality-driven design of novel functional materials, e.g., superhard, superconducting, and semiconductor materials. The electron-ion interaction was described by means of projector augmented wave (PAW)[30] with $2s^2 2p^1$, $2s^2 2p^3$ and $2s^2 2p^4$ electrons as valence for B, N and O atoms, respectively. The structural relaxations, electron localization function (ELF) and electronic band structure calculations were performed using the density functional theory within the local density approximation (LDA)[31, 32] as implemented in the Vienna *ab initio* simulation package (VASP) code.[33] The energy cutoff of 520 eV was adopted to give excellent convergence on the total energies and structural parameters. The Monkhorst-Pack (MP) k meshes[34] 0.03 $Å^{-1}$ were chosen to ensure all structures are well converged to better than 1 meV per formula. The phonon frequencies were calculated using the direct supercell method. This method uses the forces obtained by the Hellmann-Feynman theorem calculated from the optimized supercell.[35] Accurate crystal elastic constants and the modulus were calculated by the Voigt-Reuss-Hill approximation.[36] The micro-hardness model[23,37,38] based on bond strength was used for the hardness calculation. It is worth mentioning that Laplace matrix is introduced to consider the anisotropy[23] for hardness calculation. The calculations of mulliken population are carried out with the CASTEP plane-wave code.[39]

3. Results and Discussions

Variable cell simulations of B_3NO were performed at 0 ~ 100 GPa with 1 ~ 4 formula units

(f.u.) per unit cell. The calculated hardness vs. enthalpy map is shown in Fig. 1 at 0 and 100 GPa. Every point in the map represents one predicted B_3NO structure. We divide the map into four parts indicated by A, B, C and D by taking Hv = 40 GPa as the horizontal reference line and the enthalpy (−8.42 and −4.87 eV/atom for 0 and 100 GPa, respectively) of B_2O (P-4m2)[10] and c-BN[7] for the vertical reference line, which have been experimentally synthesized. Our target area is area A, which possess desirable hardness and competitive low energies. Energetically, all the structures in area A are most likely to be synthesized and might be potential superhard materials. The structures in area B are not good candidate for superhard materials, but they might also synthesizable. Structures in C and D are energetically very unfavorable and thus should be ruled out. In this work, we choose the four typical structures with negative formation enthalpies (in area A), which possess the lowest enthalpy, and the highest hardness. As shown in the Fig. 1, the most stable structure is an orthorhombic structure with $Imm2$ space group and contains 20 atoms, which is marked as oI20 (orthorhombic, $Imm2$, 20 atoms/f.u.) and the structure with the highest hardness is an orthorhombic structure $Pmm2$ (oP5). The second most stable one (orthorhombic structure with $Pmn2_1$ space group, oP20) and the one with the second-highest hardness value (hexagonal structure with $P3m1$ space group, hP5) are also studied for comparison. The enthalpy curves for these structures relative to c-BN and B_2O structure were plotted in Fig. 2. The formation enthalpy (ΔE) is defined as $\Delta E = E(B_3NO) - E(B_2O) - E(BN)$. It is clearly seen that these structures are energetically more stable than B_2O[10] and c-BN[7] at the pressures ranging from 0 to about 83 GPa. The oI20 structure is 45.3 meV per atom lower in energy than the oP20 structure at 0 GPa.

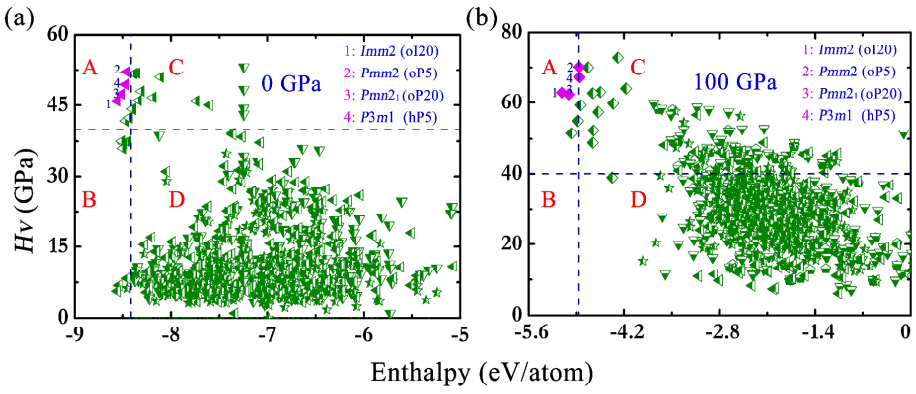

Fig. 1. The hardness vs. enthalpy map of B_3NO constructed by superhard driven calculations based on

CALYPSO method. All the predicted structures are shown at 0 GPa (a) and 100 GPa (c). Four areas indicated by A, B, C and D are divided by taking *Hv* = 40 GPa as the horizontal reference line and the total enthalpy (−8.42 eV and −4.87 eV for 0 and 100 GPa, respectively) of B_2O[10] and *c*-BN[7] for the vertical reference line.

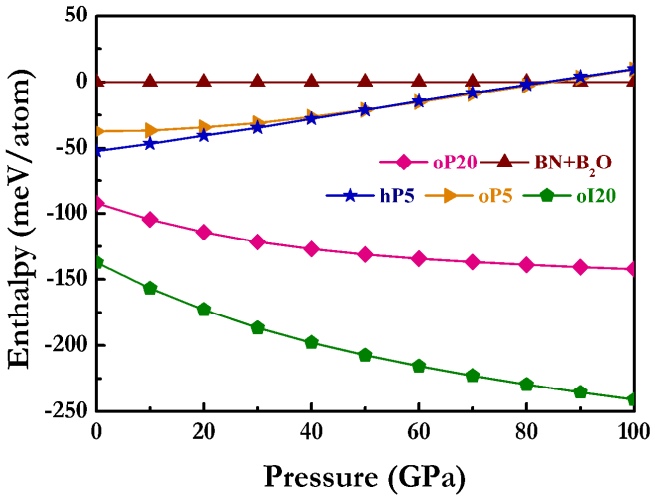

Fig. 2. Calculated enthalpy versus pressure for these representative structures relative to that of the *c*-BN[7] and B_2O[10].

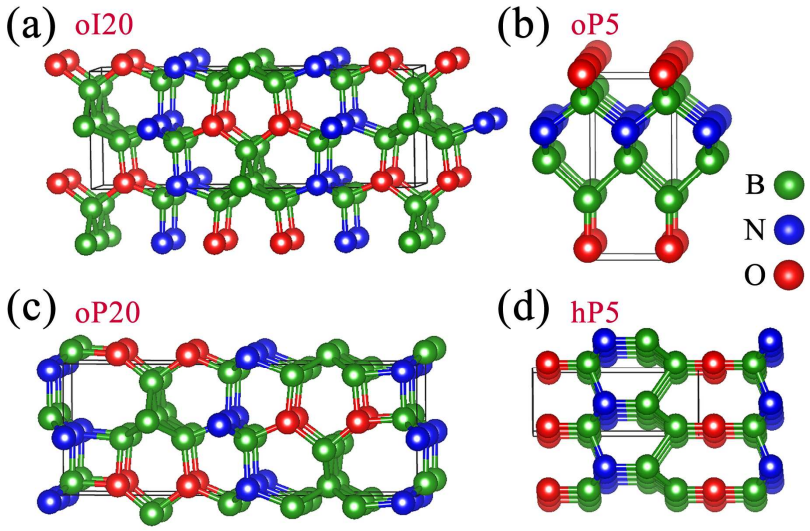

Fig.3. (color online) Structures for B_3NO: oI20 (a), oP5 (b), oP20 (c), and hP5 (d), respectively. The dark solid lines denote the unit cells. The B, N and O atoms are represented as green, blue and red spheres, respectively.

All the four structures stabilize in a three-dimensional network with typically strong covalent B-B, B-N, and B-O bonds (Fig. 3). It is found that all these structures are made up by rings with different atomic numbers. The most stable oI20 structure is comprised of irregular 6-member rings, while oP20 is formed by 4-numbered, 6-numbered, and 8-nubered rings. Both hP5 and oP5 are made up by 6- and 8- number rings. At zero pressure, for oI20 structure, the lattice parameters take a = 11.5486 Å, b = 2.5757 Å, and c = 4.1712 Å, with atomic positions of B1 at Wyckoff 2a (0, 0, 0.1567), B2 at 2b (0, 0.5, 0.4433), B3 at 4c (0.2210, 0, 0.0802), B4 at 4c (0.0899, 0, 0.5845), N at 4c (0.2165, 0, 0.4535), and O at 4c (0.3974, 0.5, 0.4440); for oP5, the lattice parameters are a = 2.5394 Å, b = 2.4362 Å, and c = 5.2887 Å, with atomic positions of B1 at 1a (0, 0, 0.0863), B2 at 1b (0, 0.5, 0.6477), B3 at 1d (0.5, 0.5, 0.4267), N at 1c (0.5, 0, 0.2500), and O at 1b (0, 0.5, 0.9224); for oP20, the lattice parameters are a = 2.5746 Å, b = 11.5431 Å, and c = 4.2533 Å, with atomic positions of B1 at 2a (0, 0.7500, 0.0747), B2 at 2a (0, 0.0243, 0.0974), B3 at 2a (0, 0.4710, 0.9354), B4 at 2a (0, 0.1646, 0.4300), B5 at 2a (0, 0.3402, 0.4297), B6 at 2a (0.5, 0.7501, 0.3605), N1 at 2a (0, 0.0271, 0.4616), N2 at 2a (0, 0.4662, 0.5619), O1 at 2a (0.5, 0.8464, 0.5768), and O2 at 2a (0.5, 0.6467, 0.5720); for hP5, the lattice parameters are a = b = 2.5915 Å, and c = 5.7107 Å, with atomic positions of B1 at 1a (0, 0, 0.8670), B2 at 1a (0, 0, 0.3382), B3 at 1b (0.3333, 0.6667, 0.6954), N at 1b (0.3333, 0.6667, 0.4373), and O at 1a (0, 0, 0.0961).

Table 1

The calculated bond length, density (ρ), bulk modulus (B), shear modulus (G) and hardness (Hv) of the predicted four typical superhard structures.

Structure	bond length (Å)			ρ	B	G	Hv
	B-O	B-N	B-B	(g/cm^3)	(GPa)	(GPa)	(GPa)
oI20	1.480, 1.507	1.558, 1.560, 1.568	1.756, 1.757	3.342	332	310	45.9
oP5	1.453, 1.495	1.535, 1.537	1.725	3.169	303	245	52.1
oP20	1.443, 1.477, 1.495	1.530, 1.549, 1.560	1.734, 1.766	3.281	326	296	47.4
	1.508, 1.529	1.572, 1.589, 1.593	1.770				
hP5	1.308, 1.383	1.474, 1.600	1.789	3.122	284	223	49.4

Table 2

The calculated elastic constants C_{ij} (GPa) of the predicted four typical superhard structures.

Structure	C_{11}	C_{22}	C_{33}	C_{44}	C_{55}	C_{66}	C_{12}	C_{13}	C_{23}
oI20	878	642	743	352	311	287	99	129	152
oP5	536	779	869	333	284	139	37	145	148
oP20	835	833	699	241	255	312	174	77	46
hP5	1422		435	140			49		

As one of the potential candidates for superhard materials, the mechanical properties of the four structures are important for the industrial applications. The calculated bond length, density (ρ), bulk modulus (B), shear modulus (G) and hardness (Hv) of these four typical structures are given in Table 1. For orthogonal and hexagonal structure, the mechanical stability requires the elastic constants satisfying the following conditions: $C_{ii}>0$ (i=1−6), $C_{11}+C_{22}+C_{33}+2(C_{12}+C_{13}+C_{23})>0$, $C_{11}+C_{22}-C_{12}>0$, $C_{11}+C_{33}-2C_{13}>0$, $C_{22}+C_{33}-C_{23}>0$, and $C_{44}>0$, $C_{11}>C_{12}$, $(C_{11}+2C_{12})*C_{33}>0$, respectively. It is clear from Table 2 that the whole set of elastic constants of these four structures satisfy the above conditions, indicating mechanical stability. The structures listed in Table 1 exhibit high bulk modulus of 284 ~ 332 GPa, indicating the structures are difficult to compress near their respective equilibrium volumes. The values have been significantly enlarged when compared to B_2O (~ 240 GPa). From the analysis of the bonding environment of these crystal structures, both B_3NO and B_2O structures adopt clear sp^3 hybridizations, but B_3NO forms additional B-N bonds besides the B-B and B-O bonds. For comparison, here we give the bond lengths of referenced B_2O[10] and c-BN[7] of 1.670 Å (B-B), 1.565 Å (B-N), 1.503, and 1.488 Å (B-O). Obviously, the B-N bond in B_3NO is much shorter than the B-B, and B-O bond in B_2O, giving stronger covalent bonds in B_3NO. The ratio between the bulk modulus (B) and shear modulus (G) can be used to predict the brittle or ductile behavior of materials. The calculated B/G for these structures reaches 1.07 ~ 1.27, which is smaller than the criteria of 1.75[40] (The ductile behavior is predicted when $B/G > 1.75$, otherwise the material behaves in a brittle manner). It is imperative to check the phonon spectra of all the four structures, since it provide crucial information on structural stabilities. No

imaginary frequency in the whole first Brillouin zone is a necessary condition to ensure the existence of the predicted structure in physics. From the calculated phonon dispersions, oI20 and oP20 [shown in Fig. 4(a), (b), respectively] are dynamically stable at 0 GPa. However, hP5 and oP5 are dynamically unstable [shown in Fig. 4(c), (d), respectively], thereby ruling out the possibility of being synthesized.

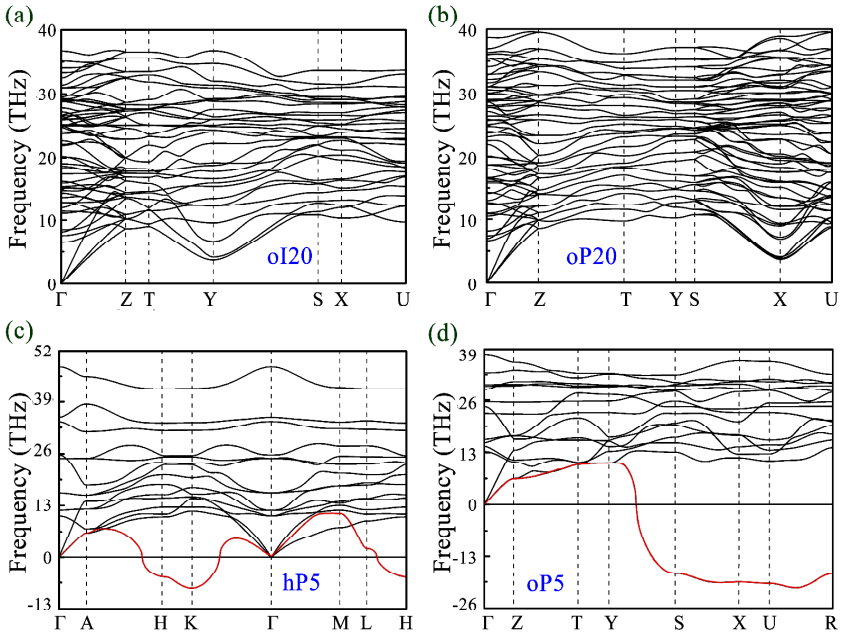

Fig. 4: The phonon dispersion of oI20 (a), oP5 (b), oP20 (c), and hP5 (d) at 0 GPa

To further understand the electronic properties, we have performed simulations on the electronic band structure and partial density of states (PDOS) of oI20 and oP20, as shown in Fig. 5. The calculated results reveal the semiconductor features of these two structures with indirect band gaps of 0.87 and 0.12 eV, respectively. Since density functional calculations typically underestimate the gap by 30% ~ 50%, the true band gap might be in the range of 1.24 ~ 1.74 eV and 0.17 ~ 0.24 eV, respectively. The electronic states near the Fermi level are mainly contributed by B-2*p* and a few N-2*p*, and O-2*p* states. The partial DOS profiles for B-2*p*, N-2*p* and O-2*p* are very similar from -12 to -4 eV, reflecting the significant hybridizations between these orbital and strong covalent interaction in both the B-N bonds and B-O bonds.

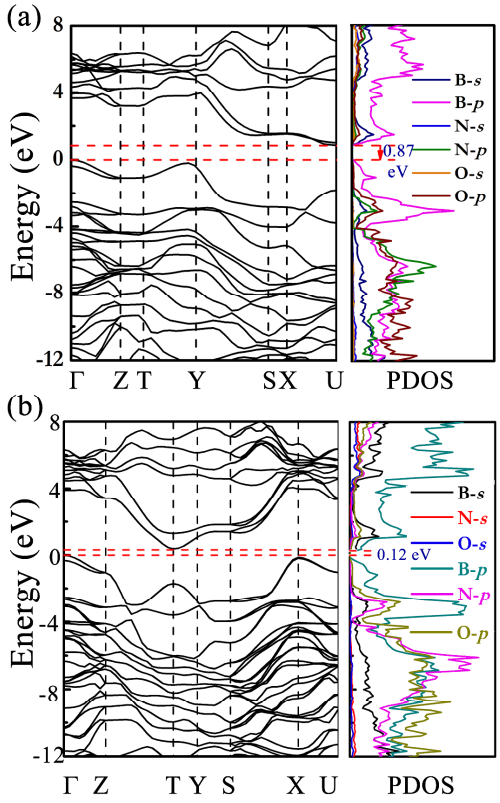

Fig. 5: (color online) Band structure (left) and the partial density of states (right) of the oI20 (a), and oP20 (b) structure at ambient pressure.

Finally, we examined the charge density distribution and the ELF that enables an effective and reliable analysis of the nature of covalent bonding. It is useful in distinguishing ionic, covalent, and metallic, bonding. Here, we use the isosurface value of 0.83 as high ELF (≥ 0.8) indicates the formation of strong covalent bonds.[41, 42] High electron localization can be seen in the region between adjacent B-B, B-N, and B-O bonds, indicative of strong covalent bonding (Fig. 6). Also the calculated overlap population of the B-B, B-N, and B-O bonds as shown in Table 3 is high, indicating that oI20 and oP20 are strong covalent solids. The calculated ELF shows that the O atoms in oI20 and oP20 structures are threefold coordinated with three near-neighbor B atoms and lone pair electrons. It is clearly seen that the electronic state is actually characterized by the 3D tetrahedral-like electronic state similar to that of the nitrogen atoms in *bct*-CN_2.[43] The N atoms are four fold-coordinated and forming a stable sp^3 bonding state. However, the bonding environment of boron atoms is more complex. Boron has three valence electrons, which is electron deficient compared with carbon. The2D, 3D ELF, and the

coordination numbers of B atoms are given in order to show a clear point of view. The B1 atoms in oI20 and B3 atoms in oP20 are six fold-coordinated with six neighboring boron atoms. Other boron atoms are four fold-coordinated and forming a stable sp^3 bonding state with boron, nitrogen and oxygen atoms. The bonding states of oI20 are similar to that of oP20 as clearly shown in 2D ELF. These strong three-dimensional covalent bonds could reasonably explain the superhardness properties of oI20 and oP20 structures. Our current research reveals that B_3NO simultaneously belongs to superhard and semiconductor materials, which may has widely application prospects in industry, such as cutting tools, coating materials, photo-catalytic materials, and so on. In addition, the present work has opened up a new route to quest functional materials.

Table 3

The calculated mulliken population of the oI20 and oP20 atructures.

oI20			oP20		
Bond	Population	Length (Å)	Bond	Population	Length (Å)
B-O	0.59	1.4802	B-O	0.64	1.4429
	0.61	1.4807		0.61	1.4774
	0.40	1.5067		0.58	1.4947
				0.53	1.4957
				0.38	1.5077
				0.42	1.5292
B-N	0.55	1.5580	B-N	0.79	1.5304
	0.58	1.5608		0.47	1.5492
	0.75	1.5681		0.58	1.5599
				0.75	1.5723
				0.55	1.5895
				0.44	1.5933
B-B	0.62	1.7560	B-B	0.64	1.7341
	0.54	1.7572		0.61	1.7664
				0.53	1.7706

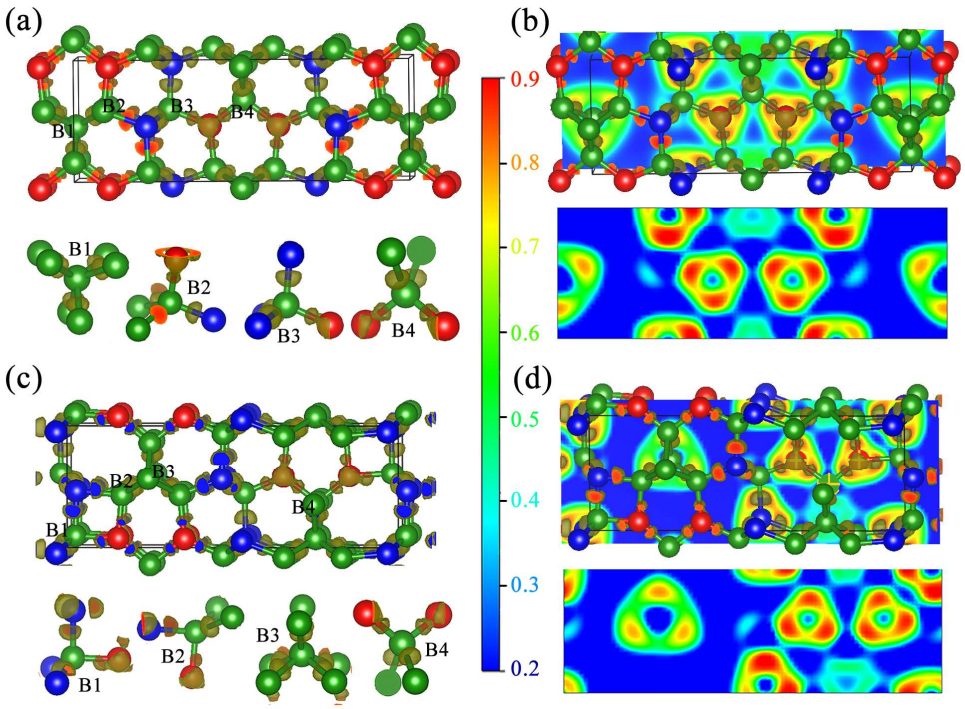

Fig. 6. (color online) Contours of the ELF of oI20 (a), (b) and oP20 (c), (d) with isosurface = 0.83. The coordination numbers of boron atoms are given for better observation.

4. Conclusions

In conclusion, we have extensively explored structures of B_3NO with a superhard-driven purpose based on CALYPSO methodology. The calculated hardness vs. enthalpy maps provide a variety of newly predicted structures of B_3NO compound contains short, strong, and three-dimensional covalent bonds. Interestingly, we uncovered two energetically stable B_3NO structures (oI20 and oP20) possessing very high hardness values. No imaginary phonon frequencies are observed indicating they are dynamically stable at 0 GPa. They are three-dimensional orthorhombic structure with space group *Imm*2 and $Pmn2_1$ (oI20 and oP20). The calculated elastic constants and modulus indicate these two structures are very incompressible as expected from their short and strong 3D chemical bonding. The calculated Vickers hardness of oI20 and oP20 phases reaches 45.9 and 47.4 GPa with an indirect band gap of 0.87 and 0.12 eV, respectively. Our current results are helpful to improve the understanding of functional-driven search and thus stimulate future experimental synthesis and determination of B_3NO.

Acknowledgements

This work is supported by the China 973 Program (2011CB808200), the Natural Science Foundation of China under 51202084, 11474125, and 11274136, the 2012 Changjiang Scholars Program of China, Changjiang Scholar and Innovative Research Team in University (IRT1132). Parts of the calculations were performed in the High Performance Computing Center (HPCC) of Jilin University.

Corresponding Author*

(Q. Li) Tel: +86-431-85167557. E-mail: liquan777@jlu.edu.cn.

References

[1] J. Bocquillon, *Annu. Rev. Mater. Sci.*, 2001, **31** , 1.
[2] V. Brazhkin, N. Dubrovinskaia, A. Nicol, N. Novikov, R. Riedel, V. Solozhenko, and Y. Zhao, *Nat. Mater.*, 2004, **3**, 576.
[3] Q. Li, H. Wang, and Y. Ma**,** *J. Superhard Mater.***,** 2010, **32**, 192.
[4] Y. Tian , B. Xu, and Z. Zhao, *Int. J. Refract Met. H.*, 2012, **33**, 93.
[5] O. O. Kurakevych, *J. Superhard Mat.*, 2009, **31**, 139.
[6] B. Xu, Y. Tian, *Sci. China Mat.*, 2015, **58**, 132.
[7] R. H. Wentorf , *J. Chem. Phys*., 1957, **26**, 956.
[8] G. M. Rignanese, J. C. Charlier, and X. Gonze, *Phys. Rev. B*, 2002, **66**, 205416.
[9] D. He, Y. Zhao, L. Daemen, J. Qian, T. D. Shen, and T. W. Zerda, *Appl. Phys. Lett.*,2002, **81**, 643.
[10] Q. Li, W. Chen, Y. Xia, Y. Liu, H. Wang, H. Wang, and Y. Ma, *Diamond Relat. Mater.,*2011, **20**, 501.
[11] Z. Pan, H. Sun, and C. Chen, *Phys. Rev. B*, 2004, **70**, 174115.
[12] Q. Li, M. Wang, Oganov A. R., T. Cui, Y. Ma, and G. Zou, *J. Appl. Phys.*,2009, **105**, 053514.
[13] S. Nakano, M. Akaishi, T. Sasaki, and S. Yamaoka, *Chem. Mater.*,1994, **6**, 2246.
[14] E. Knittle, R. B. Kaner, R. Jeanloz, and M. L. Cohen, *Phys. Rev. B*,1995, **51**, 12149.
[15] T. Komatsu, M. Nomura, Y. Kakudate, and S. Fujiwara, *J. Mater. Chem*.,1996, **6**, 1799.
[16] V. L. Solozhenko, D. Andrault, G. Fiquet, M. Mezouar and D. C. Rubie, *Appl. Phys. Lett.*, 2001, **78**, 1385.
[17] Y. Zhang, H. Sun, and C. Chen, *Phys. Rev. Lett.,* 2004, **93**, 195504.
[18] Y. Li, Q. Li, and Y. Ma , *Europhys. Lett.,* 2011, **95**, 66006.
[19] M. Zhang, H. Liu, Q. Li, B. Gao, Y. Wang, H. Li, C. Chen, and Y. Ma, *Phys. Rev. Lett.*, 2015, **114**, 015502.
[20] P. Zinin, L. Ming, H. Ishii, R. Jia, T. Acosta, and E. Hellebrand, *J. Appl. Phys.,* 2012, **111**, 114905.
[21] Y. Wang, J. Lv, L. Zhu, and Y. Ma, *Compu. Phys. Comm.,* 2012, **183**, 2063.
CALYPSO Code is Free for Academic Use. Please register at http://www.calypso.cn.

[22] Y. Wang, J. Lv and L. Zhu, and Y. Ma, *Phys. Rev. B,* 2010, **82**, 094116.
[23] X. Zhang, Y. Wang, J. Lv, C. Zhu, Q. Li, M. Zhang, Q. Li and **Y. Ma**, *J. Chem. Phys.,*2013, **138**, 114101.
[24] H. Liu and Y. Ma, *Phys. Rev. Lett.*, 2013, **110**, 025903.
[25] J. Lv, Y. Wang, L. Zhu, and Y. Ma, *Phys. Rev. Lett.,* 2011, **106**, 015503.
[26] L. Zhu, H. Wang, Y. Wang, J. Lv, Y. Ma, Q. Cui, Y. Ma, and G. Zou, *Phys. Rev. Lett.,* 2011, **106**, 145501.
[27] Q. Li, D. Zhou, W. Zheng, Y. Ma, and C. Chen, *Phys. Rev. Lett.,*2013, **110**, 136403.
[28] S. Lu, Y. Wang, H. Liu, M. Miao and Y. Ma, *Nature Commun.,*2014, **5**, 3666.
[29] L. Zhu, H. Liu, C. J. Pickard, G. Zou and Y. Ma, *Nature Chem.,* 2014, **6**, 644.
[30] G. Kresse and D. Joubert, *Phys. Rev. B*, 1999, **59**, 1758.
[31] D. M. Ceperley and B. Alder, *Phys. Rev. Lett*., 1980,**45**, 566.
[32] J. Ihm, A. Zunger, and M. L. Cohen, *J. Phys. C: Solid State Phys.*, 1979, **12**, 4409.
[33] G. Kresse and J. Furthmüller, *Phys. Rev. B*, 1996, **54**, 11169.
[34] H. J. Monkhorst and J. D. Pack, *Phys. Rev. B,* 1976, **13**, 5188.
[35] A. Togo, F. Oba, and I. Tanaka, *Phys. Rev. B*, 2008, **78**, 134106.
[36] Hill, R., *Proc. Phys. Soc.*, 1952, **65**, 349.
[37] Šimůnek and Vackář, *Phys. Rev. Lett.,*2006, **96**, 085501.
[38] Šimůnek, *Phys. Rev. B*, 2007, **75**, 172108.
[39] S. J. Clark, M. D. Segall, C. J. Pickard, P. J. Hasnip, M. I. J. Probert, K. Refson, M. C. Payne, *Z. Kristallogr.* 2005, **220**, 567.
[40] S. Pugh, *Philos. Mag.,* 1954, **45**, 823.
[41] A. D. Becke, and K. E. Edgecombe, *J. Chem. Phys.*, 1990, **92**, 5397.
[42] B. Silvi, and A. Savin, *Nature,*1994, **371**, 683.
[43] Q. Li , H. Liu , D. Zhou , W. Zheng , Z. Wu, and Y. Ma, *Phys. Chem. Chem. Phys*., 2012, **14**, 13081.